Time scales of stratified turbulent flows and relations between second-order closure parameters and flow numbers

Stefan Heinz[a)]
*Delft University of Technology, Faculty of Applied Sciences, Department of Applied Physics,
Section Heat Transfer, Lorentzweg 1, 2628 CJ Delft, The Netherlands*

The description of turbulent mixing and chemical reactions by Lagrangian probability density function methods offers some significant advantages over other methods, mainly due to the simulation of mixing processes and the exact treatment of chemical transformations. A key problem of such methods is the information on the time scales of processes, because they determine the dynamics and intensity of mixing. This question is considered for stratified flow. Different models are presented for the development of these time scales in time and their stationary spatial patterns in dependence on shear and stratification. The model predictions are shown to be in agreement with large-eddy simulations of stratified homogeneous shear flow. Two further applications of these models are considered: the description of transitions between flow regimes (characterized by different scaling quantities) in the stationary atmospheric surface layer and, second, the simulation of buoyant plume rise. It is shown that the predictions of the stationary frequency model agree with measured data. The consideration of limit cases of this model leads to connections between second-order closure parameters and (critical) flow numbers that characterize these transitions. These relationships are shown to be very advantageous for the application of closure models. A new flow number that characterizes the transition to free convective flow under unstable stratification is introduced here in analogy to the critical gradient Richardson number, which characterizes the onset of turbulence in stably stratified flow. The second application provides a new theory for buoyant plume rise. Two parameters that describe the turbulent mixing in the entrainment and extrainment stages of plume rise are explained as ratios of the relevant time scales. The two-thirds power law of buoyant plume rise, which is observed for nonturbulent and neutrally stratified flow, is obtained without having to make ad hoc assumptions. For turbulent flow, the plume's leveling-off is calculated in accord with measurements. © *1998 American Institute of Physics.*
[S1070-6631(98)02504-5]

I. INTRODUCTION

Lagrangian probability density function (PDF) methods enable a much more comprehensive description of turbulence than do two-equation or Reynolds-stress models, moreover they are still tractable computationally.[1–9] The great advantage of this approach is that it enables the exact representation of chemical reactions, which is not the case with other methods,[1] where errors of several orders of magnitude may arise from insufficient approximations.[4,8] Further, turbulent mixing (e.g., between a buoyant plume and the ambient fluid, see Sec. VI) can be described by using these methods without the need to make ad hoc assumptions on entrainment processes. This can be done by considering the motion and properties of all the fluid particles of the flow, which requires, consequently, Lagrangian equations that are consistent with Eulerian budget equations for the turbulence.

One approach to arriving at such equations is the application of partly modeled Eulerian, Reynolds-averaged, hydrodynamic equations for moments up to second order as a guideline for the derivation of the stochastic Lagrangian theory;[10–13] this means that stochastic processes that have

known Eulerian budgets are simulated. One important problem when designing such Lagrangian PDF models is the scaling of these complex interacting processes for stratified shear flows. Essentially, this problem reduces to the estimation of the dissipation time scale τ, which defines a characteristic turbulence frequency $\omega = \tau^{-1}$. When adopting the relationship between Lagrangian stochastic models and second-order moment equations, the characteristic frequencies of all the other processes are found to be proportional to ω (or they are modeled as being dependent on this quantity).[14] The same problem of estimating ω arises if a Lagrangian stochastic equation for the frequency is postulated, because the change of ω has to be specified in order to close the joint velocity–dissipation PDF equation.[15,16]

The calculation of this characteristic turbulence frequency ω (or, alternatively, of the dissipation) is a central question in second-order modeling. It is accepted that a great deal of uncertainty in respect to two-equation models or Reynolds-stress models lies in the transport equation for ω that complements these equations.[17,18] There are various methods for the estimation of ω, but these often require the solution of many complicated partial differential equations.[17,19] The consideration of temperature effects considerably increases the complexity of these equations. Thus the application of these methods to providing time scale in

a)Telephone: +31 (0)15 278 3649; Fax: +31 (0)15 278 1204; Electronic mail: heinz@wt.tn.tudelft.nl

formation for particle models would appear to be very expensive and to be related to considerable (numerical) error influences (see Sec. II B), which is of relevance in respect to efficient computation.[20]

The calculation of ω in Lagrangian PDF methods for stratified shear flows is investigated here. First, Lagrangian stochastic models and their relationship to second-order moment equations are considered. Second, a model for the time behavior of ω is presented. Its application to the simulation of developing anisotropy is addressed in Sec. III. The results are shown to be in accord with large-eddy simulation (LES) and experimental data for stratified flows. Another model for the estimation of the stationary values of ω in inhomogeneous flows is derived in Sec. IV and its predictions are compared with those of the model presented in Sec. III. In this second approach, ω is calculated as a consequence of second-order budget equations of turbulence. In Sec. V, we discuss the application of these models to the explanation of transitions between flow regimes (characterized by different scaling quantities) in the stratified atmospheric surface layer. The consideration of these transitions reveals relationships between the second-order closure parameters and flow numbers which characterize these limit cases. In Lagrangian equations, the closure parameters play a different role than they do in Eulerian transport equations for moments because they determine quantitatively the one-point joint velocity–temperature PDF.[21] Thus, these connections permit the adjustment of the turbulence statistics to specific flow characteristics. In Sec. VI, the turbulent mixing between a buoyant (stack) plume and the ambient flow is considered. Theories previously applied to this phenomenon are based on ad hoc assumptions, which is essentially related to questions of the scaling of turbulent mixing, i.e., its dependence on shear and stratification. This problem is solved here with the models presented for ω where the two-thirds power law is derived as well as (entrainment) parameters that characterize the mixing intensity and determine, e.g., the final plume height.

II. LAGRANGIAN STOCHASTIC THEORY AND TURBULENCE BUDGET EQUATIONS

A turbulent flow is considered which is described by Reynolds-averaged Navier–Stokes (RANS) equations up to second order. The turbulence budget equations (with modeled pressure redistribution and dissipation terms) are presented in Sec. II A. In Sec. II B, we consider Lagrangian equations that provide a theory of turbulence as being the stochastic motion of all the fluid particles. Eulerian transport equations for all moments of the one-point velocity–temperature PDF can be derived from these Lagrangian equations. The equations depend on the choice of coefficients in the Lagrangian equations, which are chosen here such that the Eulerian budget equations presented in Sec. II A are satisfied exactly. More details of the derivation, i.e., the estimation of coefficients, can be found elsewhere, together with a discussion of different equation types and the relations to approaches applied previously.[13] The Lagrangian equations presented in Sec. II B reveal, in particular, the relevance of models for the turbulence frequency ω.

A. Turbulence budget equations

The Eulerian (subscript E) velocity $\mathbf{U}_E(\mathbf{x},t)$ and potential temperature $\Theta_E(\mathbf{x},t)$ at the position $\mathbf{x}=(x^1,x^2,x^3)$ and time t are considered together in a four-dimensional state vector $\mathbf{Z}_E(\mathbf{x},t)=[\mathbf{U}_E(\mathbf{x},t),\Theta_E(\mathbf{x},t)]$. The ensemble average of the component k of $\mathbf{Z}_E$ is denoted by $\langle Z_E^k\rangle$, and $z=\mathbf{Z}_E-\langle \mathbf{Z}_E\rangle=(u,\theta)$ are the fluctuations. The equations for the mean fields $\langle Z_E^k\rangle$ are not presented here[13] because they are not essential to the analysis below. All the variances of the velocity and potential temperature fields are described as elements of the matrix of second moments

$$V=\begin{vmatrix} \langle u^1u^1\rangle & \langle u^1u^2\rangle & \langle u^1u^3\rangle & \langle u^1\theta\rangle \\ \langle u^2u^1\rangle & \langle u^2u^2\rangle & \langle u^2u^3\rangle & \langle u^2\theta\rangle \\ \langle u^3u^1\rangle & \langle u^3u^2\rangle & \langle u^3u^3\rangle & \langle u^3\theta\rangle \\ \langle \theta u^1\rangle & \langle \theta u^2\rangle & \langle \theta u^3\rangle & \langle \theta^2\rangle \end{vmatrix}. \tag{1}$$

The elements of V are denoted by small superscripts if they run from 1 to 4 and by capital superscripts if they run only over velocity components from 1 to 3. The transport equations for the moments of second-order V^{ij} are considered in an approximation for the dissipation according to Kolmogorov's theory[22] and Rotta's[23] approximation of a return-to-isotropy pressure redistribution is applied as a simple example. The sum V^{KK} over velocity autovariances gives twice the turbulent kinetic energy (TKE) $q^2=V^{KK}$ (summation over repeated superscripts is assumed) and the ratio $\tau=q^2/(2\epsilon)$ defines a dissipation time scale τ, where ϵ denotes the mean dissipation rate of TKE. The inverse time scale τ gives the turbulence frequency $\omega=\tau^{-1}$. The second-order moment equations may then be written[13]

$$\frac{DV^{ij}}{Dt}+R^{ij}+P^{ij}$$

$$=-\frac{k_1}{2\tau}\left(V^{ij}-\frac{q^2}{3}\delta_{ij}\right)+\left[\beta g\delta_{i3}+\frac{k_1-k_3}{2\tau}\delta_{i4}\right]V^{4j}$$

$$+\left[\beta g\delta_{j3}+\frac{k_1-k_3}{2\tau}\delta_{j4}\right]V^{4i}$$

$$-\frac{(k_1-2)/3\cdot q^2-(2k_3-2k_4-k_1)V^{44}}{2\tau}$$

$$\times\delta_{i4}\delta_{j4}-\frac{q^2}{3\tau}\delta_{ij}, \tag{2}$$

where the Boussinesq approximation and the incompressibility constraint are applied. Here, the operator $D/Dt(\cdot)=[\partial/\partial t+\partial/\partial x^K\langle Z_E^K\rangle](\cdot)$ is used, β is the thermal expansion coefficient, and g is the acceleration due to gravity. The equation system (2) is not closed because the gradients of triple correlations $R^{ij}=\partial\langle z^K z^i z^j\rangle/\partial x^K$ appear as unknown terms. This closure problem is not considered here because it does not play any role in the derivation of the Lagrangian theory considered next. The production $P^{ij}=\langle z^K z^i\rangle\partial\langle Z_E^j\rangle/\partial x^K+\langle z^K z^j\rangle\partial\langle Z_E^i\rangle/\partial x^K$ is proportional to the gradients $\partial\langle Z_E^J\rangle/\partial x^K$ of the mean velocity ($J=1,2,3$), but it is also proportional to the gradients $\partial\langle Z_E^4\rangle/\partial x^K$ of the potential temperature field. Only the terms on the right-hand side of (2),

which represent the redistribution and dissipation, are modeled. The closure parameters k_1 and k_3 arise from Rotta's return-to-isotropy theory,[23] and k_4 describes the ratio of the time scales for the dissipation of TKE to that of the potential temperature variance. A variety of different estimates for these closure parameters can be found in the literature, as discussed in Sec. V. These parametrizations agree with those applied, e.g., by Launder,[24] with the exception of the rapid pressure term (proportional to a very small parameter k_2, see Sec. V), which is neglected here together with a corresponding term in the heat flux equation.[13] This model is the simplest possible for the return to isotropy,[10,25] where the whole of the redistribution is modeled by the slow pressure fluctuations. The contributions of other terms can be partly compensated for by variations of the values for the closure parameters.[26] The simplicity of Eq. (2) makes it well suited to a demonstration of the way in which such equations can be applied as guidelines for the development of a Lagrangian theory.

Equation (2) requires one important additional ingredient: a model for the calculation of the turbulence frequency $\omega = \tau^{-1}$ that determines the scale of the turbulence. The development of equations for ω and some related questions have been reviewed, e.g., by Wilcox. He presents as a state-of-the-art formulation of such an equation[17,19]

$$\frac{D}{Dt}\omega = -\omega^2 \left\{ (C_{\epsilon 2}-1) - (C_{\epsilon 1}-1)\frac{P}{\epsilon} \right\}$$
$$+ \frac{\partial}{\partial x^j}\left[\left(\nu + \sigma C_\mu \frac{q^2}{2\omega}\right)\frac{\partial \omega}{\partial x^j}\right], \tag{3}$$

where P is the production of TKE, $C_{\epsilon 1}$, $C_{\epsilon 2}$, C_μ, and σ are constants (their estimation is discussed by Wilcox, standard values are $C_{\epsilon 1}=1.56$, $C_{\epsilon 2}=1.9$, $C_\mu=0.09$, and $\sigma=0.5$) and ν is the kinematic molecular viscosity. The production–dissipation ratio of TKE, $P = -P^{LL}/2 + \beta g V^{34}$ to $\epsilon = q^2/(2\tau)$, can be obtained by adopting the definition of $P^{LL} = 2\langle z^K z^L \rangle \partial \langle Z_E^L \rangle / \partial x^K$ as

$$\frac{P}{\epsilon} = \frac{2\tau}{q^2}\left\{ -V^{KL}\frac{\partial \langle Z_E^L \rangle}{\partial x^K} + \beta g V^{34} \right\}, \tag{4}$$

which also contains terms related to the buoyancy production. The model (3) is denoted the basic frequency model (BFM). This equation is postulated in a formal analogy to transport equations for the TKE. The terms on the right-hand side of (3) represent the main processes that cause changes of ω in space and time: dissipation (the first term), production (the second term), and diffusion (the third and fourth terms). This model plays an essential part in the following explanations because it represents (due to the relationships between the Eulerian and Lagrangian theory) one way to determine the time scales in Lagrangian PDF methods. This is discussed in Sec. II B in conjunction with the presentation of the Lagrangian theory.

B. Lagrangian stochastic theory

The flow considered in Sec. II A is now described in the Lagrangian framework. A Lagrangian theory that is fully consistent with the equations for the mean velocities and

temperatures and the turbulence budget equations (2) can be derived by considering linear equations for the stochastic process $\mathbf{Z}_L(t) = [\mathbf{U}_L(t), \Theta_L(t)]$, where $\mathbf{U}_L(t)$ and $\Theta_L(t)$ are fluid particle velocities and potential temperature (the subscript L denotes a Lagrangian quantity), respectively. Such equations may be written as (I runs again from 1 to 3 in contrast to i)

$$\frac{d}{dt}x_L^I(t) = Z_L^I(t), \tag{5a}$$

$$\frac{d}{dt}Z_L^i(t) = \langle a^i \rangle + G^{ij}(Z_L^j - \langle Z_E^j \rangle) + b^{ij}\frac{dW^j}{dt}, \tag{5b}$$

where dW^j/dt is a Gaussian process with vanishing mean values, $\langle dW^j/dt \rangle = 0$, and with uncorrelated values at different times, $\langle dW^i/dt(t) \cdot dW^j/dt'(t') \rangle = \delta_{ij}\delta(t-t')$. The symbol δ_{ij} is the Kronecker delta and $\delta(t-t')$ is the delta function. This approach permits the derivation of Lagrangian equations which are explicit in the velocities and temperatures. This is in contrast to approaches[3,13] that are aimed at the consistency of the Lagrangian theory with evolution equations for the one-point joint velocity–temperature PDF of the flow. The latter require information on this PDF, which is a nontrivial problem that has previously been handled by empirical methods.[9]

The constraint of consistency between the averaged conservation equations for momentum and potential temperature derived from (5a) and (5b) and those obtained within the Eulerian closure theory determines $\langle a^i \rangle$. The variance equations derived from (5a) and (5b) are identical to Eq. (2), if the matrix b is determined by[13]

$$B = \frac{1}{4\tau}\begin{pmatrix} C_0 q^2 & 0 & 0 & 0 \\ 0 & C_0 q^2 & 0 & 0 \\ 0 & 0 & C_0 q^2 & 0 \\ 0 & 0 & 0 & C_1 \langle \theta^2 \rangle \end{pmatrix}, \tag{6a}$$

where $B^{ij} = \frac{1}{2}b^{ik}b^{kj}$, and, if the matrix G is given by

$$G^{ij} = -\frac{k_1}{4\tau}\delta_{ij} + \frac{k_1-k_3}{2\tau}\delta_{i4}\delta_{j4} + \beta g \delta_{i3}\delta_{j4}. \tag{6b}$$

The constants in (6a) depend on the closure parameters, $C_0 = (k_1-2)/3$ and $C_1 = 2k_3 - 2k_4 - k_1$. A discussion of the nonuniqueness of G can be found elsewhere.[13] Additional constraints are required [e.g., to correlations $\langle dZ_L^i(t)/dt\, Z_L^j(t) \rangle$ with $i \neq j$] in order to estimate G completely but these influences can be neglected in many applications. The construction of these Lagrangian equations (5a) and (5b) confirms the realizability of the second-order moment equation (2) provided that the coefficients $\langle a^i \rangle$, G^{ij}, and b^{ij} are bounded. We note that these variance equations are reproduced without any assumptions about the transport terms R^{ij}. Hence, the incorporation of information on the time scale τ is most essential for the Lagrangian equations. This means that these equations depend on τ and the closure parameters k_1, k_3, and k_4 if mean quantities are derived from particle properties.[1,7,13]

The application of the BFM to the modeling of τ in Lagrangian PDF methods would be related to different problems. First, Eqs. (3) and (4) combined with (2) are not closed because of the appearance of the triple correlation gradients in the Eulerian transport equation (2). Second, the spatial transport terms in (3) and in Eq. (2) would represent "Eulerian elements" in a Lagrangian theory of the turbulent flow, which would cause a considerable computational effort and corresponding numerical problems. Third, the formulation of the spatial gradient terms on the right-hand side of (3) cannot be seen to be better founded than other choices. With the same argument to represent the influence of the main processes, one can postulate transport equations similar to (3) for ϵ (recent developments of models for the TKE dissipation rate have been reviewed, e.g., by Hanjalić[27] or for ω^2.[17,19] The transformation of these equations into transport equations for ω recovers the dissipation and production terms on the right-hand side of (3), but different spatial transport terms are obtained.

Thus, to provide a time scale determining equation for particle methods for stratified flow two methods are considered below. The first approach neglects the "Eulerian elements" in the BFM (3), i.e., the spatial transport terms. This model for the development of the turbulence frequency ω in time is investigated in Sec. III and applied to the calculation of the buoyant plume rise in Sec. VI. The stationary spatial patterns of ω are calculated in the second approach without reference to the BFM as a consequence of turbulence equation (2). This is explained in Sec. IV and implications for the description of the atmospheric surface layer are considered in Sec. V.

III. THE HOMOGENEOUS FREQUENCY MODEL

In Sec. III A, the BFM (3) is considered for a horizontally homogeneous flow with a stationary forcing by shear and stratification. This specification illustrates in more detail the problems that would be related to its application in particle methods for stratified flow. The above-described first approach to solving these questions is then developed in Sec. III B, where the BFM is simplified.

A. The BFM for a flow with stationary forcing

As is often done in geophysical applications, we consider a horizontally homogeneous flow with a mean horizontal velocity U along the x^1 axis. The mean flow is considered to be stationary, such that it depends only on the vertical coordinate x^3, i.e., $\langle \mathbf{Z}_E \rangle = [U(x^3), 0, W, \Theta(x^3)]$. Here, W is the mean vertical velocity, which is constant due to the incompressibility constraint, and Θ is written for the mean Eulerian potential temperature. This assumed stationarity simplifies the explanations and comparisons given below and it provides a sufficient frame for all the flows considered: homogeneous shear flow, the stationary atmospheric boundary layer, and the buoyant plume rise, where the changes of the turbulence in time (which are determined by ω) are considered to be much faster than those of the mean fields.[28] These assumptions in respect to the mean fields provide stationary time scales that describe the forcing by shear and stratification (see Sec. V A), $\tau_U = [\partial U/\partial x^3]^{-1}$ and $\tau_\Theta = |\beta g \, \partial \Theta/\partial x^3|^{-1/2}$, respectively.

The evolution of the dissipation time scale τ forced by τ_U and τ_Θ is described by the BFM (3) combined with the turbulence equation (2). It is advantageous to consider a combination of t and τ with the mean velocity gradient; i.e., $t' = t(\partial U/\partial x^3)$ and the dimensionless time scale $T = \tau(\partial U/\partial x^3)$ are introduced. The couplings in Eq. (2) are reduced for the flow under consideration and one obtains for the variances the equation system

$$
\frac{D}{Dt'}
\begin{pmatrix}
\hat{V}^{13} \\ \hat{V}^{14} \\ \hat{V}^{34} \\ \hat{V}^{33} \\ \hat{V}^{44} \\ \hat{q}^2
\end{pmatrix}
+
\begin{pmatrix}
\hat{R}^{13} \\ \hat{R}^{14} \\ \hat{R}^{34} \\ \hat{R}^{33} \\ \hat{R}^{44} \\ \hat{R}^{KK}
\end{pmatrix}
= \frac{1}{T}
\begin{pmatrix}
-k_1/2 & T & 0 & -T & 0 & 0 \\
-\mathrm{Ri}T & -k_3/2 & -T & 0 & 0 & 0 \\
0 & 0 & -k_3/2 & -\mathrm{Ri}T & T & 0 \\
0 & 0 & 2T & -k_1/2 & 0 & (k_1-2)/6 \\
0 & 0 & -2\mathrm{Ri}T & 0 & -k_4 & 0 \\
-2T & 0 & 2T & 0 & 0 & -1
\end{pmatrix}
\begin{pmatrix}
\hat{V}^{13} \\ \hat{V}^{14} \\ \hat{V}^{34} \\ \hat{V}^{33} \\ \hat{V}^{44} \\ \hat{q}^2
\end{pmatrix},
\tag{7}
$$

where the operator $D/Dt'(\cdot) = [\partial/\partial t' + W(\partial U/\partial x^3)^{-1} \times \partial/\partial x^3](\cdot)$ and the gradient Richardson number $\mathrm{Ri} = [\beta g \, \partial \Theta/\partial x^3]/[\partial U/\partial x^3]^2$ are used. The matrix V of second-order moments and the matrix R of gradients of third-order moments are here modified to

$$
\hat{V} = \frac{1}{q_0^2}
\begin{pmatrix}
\langle u^1 u^1 \rangle & \langle u^1 u^2 \rangle & \langle u^1 u^3 \rangle & \chi \langle u^1 \theta \rangle \\
\langle u^2 u^1 \rangle & \langle u^2 u^2 \rangle & \langle u^2 u^3 \rangle & \chi \langle u^2 \theta \rangle \\
\langle u^3 u^1 \rangle & \langle u^3 u^2 \rangle & \langle u^3 u^3 \rangle & \chi \langle u^3 \theta \rangle \\
\chi \langle \theta u^1 \rangle & \chi \langle \theta u^2 \rangle & \chi \langle \theta u^3 \rangle & \chi^2 \langle \theta^2 \rangle
\end{pmatrix},
$$

$$
\hat{R} = \frac{1}{q_0^2}
\begin{pmatrix}
\hat{R}^{11} & \hat{R}^{12} & \hat{R}^{13} & \chi \hat{R}^{14} \\
\hat{R}^{21} & \hat{R}^{22} & \hat{R}^{23} & \chi \hat{R}^{24} \\
\hat{R}^{31} & \hat{R}^{32} & \hat{R}^{33} & \chi \hat{R}^{34} \\
\chi \hat{R}^{41} & \chi \hat{R}^{42} & \chi \hat{R}^{43} & \chi^2 \hat{R}^{44}
\end{pmatrix},
\tag{8}
$$

such that all elements of $\hat{V}$ and $\hat{R}$ are dimensionless. These quantities as well as $\hat{q}^2 = q^2/q_0^2$ are normalized to the initial value of twice the TKE q_0^2, and the abbreviation $\chi = \beta g (\partial U/\partial x^3)^{-1}$ is applied in (8). The equation for $\hat{V}^{11}$ reads

$$\frac{D\hat{V}^{11}}{Dt'} + \hat{R}^{11} = -\frac{k_1}{2T}\hat{V}^{11} - 2\hat{V}^{13} + \frac{k_1-2}{6T}\hat{q}^2, \tag{9}$$

which is coupled with (7) via $\hat{q}^2$ and $\hat{V}^{13}$. The $\hat{V}^{22}$ are determined by $\hat{V}^{22} = \hat{q}^2 - \hat{V}^{33} - \hat{V}^{11}$, and the remaining components of $\hat{V}$ satisfy

$$\frac{D}{Dt'}\begin{pmatrix}\hat{V}^{12}\\\hat{V}^{23}\\\hat{V}^{24}\end{pmatrix} + \begin{pmatrix}\hat{R}^{12}\\\hat{R}^{23}\\\hat{R}^{24}\end{pmatrix} = \frac{1}{T}\begin{pmatrix}-k_1/2 & -T & 0\\0 & -k_1/2 & 1\\0 & -\mathrm{Ri}T & -k_3/2\end{pmatrix}$$
$$\times\begin{pmatrix}\hat{V}^{12}\\\hat{V}^{23}\\\hat{V}^{24}\end{pmatrix}. \tag{10}$$

Consequently, the estimation of τ through the BFM (3) coupled with (7) requires, even for this simplified flow, the solution of seven partial differential equations and information about the gradients of third-order terms, which are essential ingredients of turbulence models for stratified flow.[21] This effort to provide τ for Lagrangian particle methods (and the related influences of numerical errors) is in obvious contradiction with the practical requirements for calculations where, e.g., a detailed chemistry is additionally considered. Moreover, there are unsolved questions as to the justification of the spatial transport terms on the right-hand side of (3) as discussed above.

B. The homogeneous frequency model

We now consider an approximation where the spatial transport terms of ω are neglected in the BFM (3). Correspondingly, the influence of all the other ''Eulerian elements'' (the spatial transport terms of the variances $\hat{V}$ and the gradients of triple correlations $\hat{R}$) on the estimation of ω is also neglected in Eq. (7). The BFM (3) then reads

$$\frac{d}{dt'} T = (C_{\epsilon2} - 1) - (C_{\epsilon1} - 1)2T\left\{-\frac{\hat{V}^{13}}{\hat{q}^2} + \frac{\hat{V}^{34}}{\hat{q}^2}\right\}. \tag{11}$$

This model is denoted the homogeneous frequency model (HFM) because of the neglect of spatial transport terms. By adopting the definition (4) of P/ϵ, this relation can also be written as $dT/dt' = (C_{\epsilon2} - 1) - P/\epsilon \cdot (C_{\epsilon1} - 1)$. Hence, T changes as long as the dissipation and production do not balance each other. If the dissipation time scale reaches a stationary balance with the time scale of forcing $\tau_U = [\partial U/\partial x^3]^{-1}$, i.e., if T becomes constant, relation (11) provides a constant asymptotic value $p = (C_{\epsilon2} - 1)/(C_{\epsilon1} - 1)$ of P/ϵ. The values given above for $C_{\epsilon1}$ and $C_{\epsilon2}$ yield $p = 1.6$, which is a typical value for a homogeneous shear flow.[29]

Consequently, turbulent flows can be described by the HFM (11) where P/ϵ becomes constant asymptotically. This is ensured at least for two benchmark turbulent flows: an homogeneous shear flow and the logarithmic layer of an equilibrium turbulent boundary layer. The first flow constitutes a basic building-block for free turbulent shear flows and the latter flow serves as a cornerstone for the calculation of practical wall-bounded turbulent flows of engineering and

environmental interest.[29] This condition permits the application of the PDF approach to stratified geophysical flows (the atmospheric boundary layer, for instance), where similar assumptions are often applied.[30,31]

In Sec. VI, we discuss Eq. (11) in relation to its application to the explanation of buoyant plume rise. It is important to note that the consideration of combinations of ω with the shear $\partial U/\partial x^3$ permits the calculation of the time development and spatial patterns of $\omega = (\partial U/\partial x^3)/T(\mathrm{Ri}, t\partial U/\partial x^3)$ in dependence on the vertical profiles of shear and stratification. This is illustrated below where the same ω as provided by the BFM is obtained by means of (11) for a flow with a logarithmic mean velocity profile. This approach can be also applied to unsheared turbulence. This is demonstrated in respect to buoyant plume rise and in Sec. V, where we show that the stationary ω combines then with the vertical temperature gradient.

This frequency model differs from that applied by Pope[16] for a neutrally stratified inhomogeneous flow because of the couplings with the second-order equation (7). In his model, the ω equation is decoupled from the variance equations by the assumption that the turbulent shear stress $\hat{V}^{13}$ is related to the mean strain rate via a turbulent viscosity, $\hat{V}^{13} = -C_\mu q^2 T/2$,[32,33] with $C_\mu = 0.09$ as above (the vertical heat flux $\hat{V}^{34}$ is equal to zero under these conditions). In order to assess the performance of a comparable simplification of the complex calculation of T, let us consider a model where the second term on the right-hand side of (11) is proportional to T^2, i.e.,

$$\frac{d}{dt'} T = (C_{\epsilon2} - 1) - C(C_{\epsilon1} - 1)T^2. \tag{12}$$

By applying the parametrization $\hat{V}^{13} = -C_\mu q^2 T/2$ in (11) one can see that C is equal to C_μ under neutral stratification where $\hat{V}^{34}$ disappears. The introduced parameter C determines the asymptotic value T_∞ of T, since $C = (C_{\epsilon2} - 1)/(C_{\epsilon1} - 1)\cdot T_\infty^{-2}$. Hence, C depends on the stratification because T_∞ varies strongly with it (see below). In order to take this variation into account, let us apply the relation between C and T_∞ for the estimation of C, where T_∞ is assumed to be known (e.g., through the approach presented in Sec. IV). Then, (12) becomes

$$\frac{d}{dt'} T = (C_{\epsilon2} - 1)\{1 - T^2/T_\infty^2\}. \tag{13}$$

This equation is solved by (I is the initial value of T at $t = 0$)

$$T = T_\infty \frac{T_\infty/I + 1 - (T_\infty/I - 1)\exp\{-2(C_{\epsilon2} - 1)t'/T_\infty\}}{T_\infty/I + 1 + (T_\infty/I - 1)\exp\{-2(C_{\epsilon2} - 1)t'/T_\infty\}}. \tag{14}$$

Model (14) is denoted the simplified homogeneous frequency model (SHFM).

The time scale T calculated by the HFM and the SHFM is shown in Figs. 1 and 2 for different stratified flows and different values of the asymptotic production–dissipation ratio of TKE p. This is done for the HFM by solving the coupled equation system (7) and (11) by a Runge–Kutta pro-
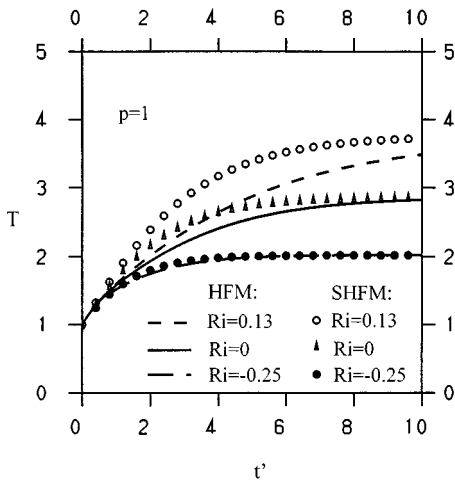
FIG. 1. The development of the normalized time scale $T = \tau \partial U / \partial x^3$ in the normalized time $t' = t \partial U / \partial x^3$ as obtained by the HFM and the SHFM for different stratified flows and an asymptotic production–dissipation ratio of TKE $p = 1$.

FIG. 3. The development of anisotropy in the components A^{11} and A^{13} of the anisotropy tensor for different values of the gradient Richardson number Ri where $p = 1.6$.

cedure with the initial conditions $\hat{V}^{ij} = 1/3 \cdot \delta_{ij}$ and $T(t=0) = I = 1$, i.e., the development of anisotropy is considered for an initially isotropic flow. The chosen initial value of $\hat{V}^{44}$ has only a negligible influence on the calculated curves. The values $p = 1$ and $p = 1.6$ are considered because they are known to characterize the stationary features of the logarithmic layer of an equilibrium turbulent boundary layer and an homogeneous shear flow, respectively.[29] The parameters k_1, k_3, and k_4 are given by standard values: k_1 was set to 8.3,[10] $k_3 = 6.14$ provides the ratio $k_3/k_1 = 0.74$, and $k_4 = 3.76$ provides a critical gradient Richardson number of 0.21 (see Sec. V). The chosen value of Ri at unstable stratification corresponds with that of Ri_0 (see also Sec. V) and Ri$=0.13$ was used for LES by Kaltenbach et al.[34] These curves show that the time scale T decreases with growing instability of the flow (i.e., for smaller Ri). For constant shear $\partial U / \partial x^3$, this result confirms the expectation that the time scale $\tau = q^2/(2\epsilon)$ of the TKE dissipation becomes smaller with in-
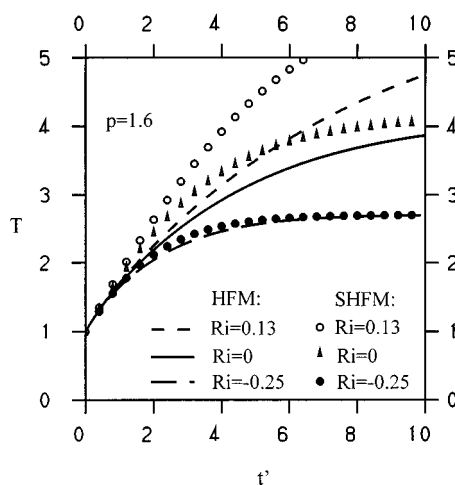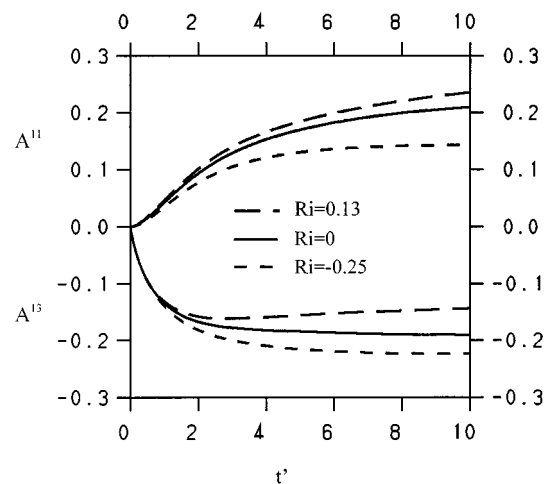
creasing intensity of turbulence. T grows with a higher production (for a higher p) because it is proportional to the shear. Although the SHFM has the same initial and asymptotic values (these are taken here from the HFM, but they can also be estimated independently, as demonstrated in Sec. IV) as the HFM, there can be considerable differences at intermediate times. The differences are relatively small for unstably and neutrally stratified flows; however the deviation is larger for stable stratification.

For the homogeneous shear flow ($p = 1.6$), the time behavior of the components A^{11} and A^{13} of the tensor of anisotropy $A^{ij} = V^{ij}/q^2 - 1/3 \cdot \delta_{ij}$ is shown in Fig. 3. The curves of the time scale T are given in Fig. 2 for the same stratifications. The dynamic behavior is in agreement with LES and direct numerical simulation (DNS) data which show that the asymptotic stage is reached if about $t' > 6$.[34,35] The investigation by experiment of the features of the asymptotic stage provides relatively accurate data only for unstratified shear flows. This knowledge was obtained in wind-tunnel studies and has been summarized by Tavoularis and Karnik.[36] Stratified flow experiments provide a considerable scatter of measured data;[37,38,24] more precise estimations are provided by DNS and LES data.[34,35] In Table I, the findings for the asymptotic values of A^{ij}, the correlation coefficients $\rho^{ij} = \hat{V}^{ij}/\sqrt{\hat{V}^{ii}\hat{V}^{jj}}$ (without summation over repeated indices here), and the ratio V^{34}/V^{14} obtained with the HFM are compared to Tavoularis and Karnik's results and LES data (DNS data provide very similar results if the strength of stratification is not too high) that are available for neutrally and stably stratified flows.[34] The data calculated by the HFM are at least qualitatively in a good agreement with the results of experiments and the LES data. It is worth emphasizing that standard values are used for the parameters k_1, k_3, and k_4 for this comparison, i.e., they are not fitted to, e.g., the LES data. The anisotropy is somewhat overestimated by the HFM and the T obtained is somewhat too small. However, it must be noted that these LES data present mean values in space that vary in time, e.g., by 3%. The relation between T and the

FIG. 2. The same curves as in Fig. 1, but now for $p = 1.6$.

TABLE I. The normalized time scale T, elements of the anisotropy tensor and correlation coefficients calculated by the HFM and LES for different gradient Richardson numbers Ri, where $r_i = \mathrm{Ri}/|\mathrm{Ri}|$ is used. The results of Tavoularis and Karnik's (Ref. 36) measurements (abbreviated as TK) at Ri$=0$ are also shown.

Ri	-0.25	0			0.13	
	HFM	HFM	TK	LES	HFM	LES
T	2.71	4.15	4.5	5.0	8.12	5.7
A^{11}	0.144	0.225	0.18	0.184	0.296	0.220
$-A^{22}$	0.112	0.112	0.06	0.033	0.112	0.036
$-A^{33}$	0.032	0.112	0.11	0.150	0.183	0.184
$-A^{13}$	0.225	0.193	0.16	0.151	0.119	0.105
$-\rho^{13}$	0.593	0.549	0.48	0.493	0.388	0.365
ρ^{14}/r_i	0.914	0.970	$\cdots$	0.600	1.007	0.603
$-\rho^{34}/r_i$	0.874	0.769	$\cdots$	0.467	0.534	0.323
$-V^{34}/V^{14}$	0.761	0.499	$\cdots$	0.480	0.259	0.282

elements of the anisotropy tensor is demonstrated in Sec. V in relation to the investigation of the effect of flow number variations. These results confirm the idea that the time scale of the TKE dissipation becomes smaller (i.e., T also becomes smaller for approximately constant shear) if the anisotropy becomes stronger. A corresponding adjustment between the results of the HFM and the experimental results and LES data provides much better agreement. The equality of the components A^{22} and A^{33} at Ri$=0$ is caused by the neglect of rapid pressure terms in the HFM. Nevertheless, these terms are also dropped in the following sections because our primary interest is in the time scale estimation.

IV. THE STATIONARY FREQUENCY MODEL

The HFM explains the variation of the dissipation time scale τ with changes of turbulence, which is represented by the variance terms in (11). Under stationary conditions, this model provides for the dependence of the normalized time scale $T = \tau(\partial U/\partial x^3)$ on the turbulence

$$p = 2T\left\{ -\frac{\hat{V}^{13}}{\hat{q}^2} + \frac{\hat{V}^{34}}{\hat{q}^2} \right\}, \tag{15}$$

where $p = (C_{\epsilon 2} - 1)/(C_{\epsilon 1} - 1)$ is the stationary value of P/ϵ. This relation corresponds to (4) for the considered flow, i.e., it can also be obtained as a consequence of the definitions of P, $\epsilon = q^2/(2\tau)$, as well as for T and $\hat{V}$. Consequently, the dependence of T on the turbulence (i.e., on the normalized variances in the brackets) is determined under stationary conditions through (15) if p is given. It is worth emphasizing that no reference is made here to the BFM or HFM. By

calculating the variances in (15) by means of the second-order moment equation (7) for the same flow as that considered in Sec. III, one can derive an equation for the asymptotic values of T. This is now done in order to further assess the results obtained in Sec. III. The value p has to be given also in the above-described approach, where it is determined by the choice of $C_{\epsilon 1}$ and $C_{\epsilon 2}$. Thus, the approach developed below can be applied under the same conditions as the HFM, this means at least for a homogeneous shear flow and the logarithmic layer of an equilibrium turbulent boundary layer.

In Sec. IV A, the second-order moment transport equation (7) is used for the calculation of the variances in (15) in dependence on T. In Sec. IV B, this relation is converted into an equation for T and its predictions are compared to the stationary values provided by the HFM. Such spatial patterns of the ω field are important in many geophysical applications where stratification effects may lead to ω variations over several orders of magnitude. Because of the lack of other concepts, these effects are often included in an ad hoc way in frequency calculations for dispersion models.[39]

A. The production−dissipation ratio of TKE

Relation (15) for T can be made much more explicit by adopting Eq. (7) for the calculation of the variances $\hat{V}^{13}/\hat{q}^2$ and $\hat{V}^{34}/\hat{q}^2$. For the flow under consideration, these equations are only a consequence of the applied pressure and dissipation parametrizations. The asymptotic variance values are determined according to Eq. (7) by

$$
\begin{pmatrix} d^{13} \\ d^{14} \\ d^{34} \\ d^{33} - (k_1 - 2)/(6T) \\ d^{44} \end{pmatrix} =
\begin{pmatrix}
-k_1/(2T) & 1 & 0 & -1 & 0 \\
-\mathrm{Ri} & -k_3/(2T) & -1 & 0 & 0 \\
0 & 0 & -k_3/(2T) & -\mathrm{Ri} & 1 \\
0 & 0 & 2 & -k_1/(2T) & 0 \\
0 & 0 & -2\mathrm{Ri} & 0 & -k_4/T
\end{pmatrix}
\begin{pmatrix} \hat{V}^{13}/\hat{q}^2 \\ \hat{V}^{14}/\hat{q}^2 \\ \hat{V}^{34}/\hat{q}^2 \\ \hat{V}^{33}/\hat{q}^2 \\ \hat{V}^{44}/\hat{q}^2 \end{pmatrix}. \tag{16}
$$

Here, the abbreviations $d^{ij} = [D\hat{V}^{ij}/Dt' + \hat{R}^{ij}]\hat{q}^{-2}$ are introduced for the transport terms. The calculation of $\hat{V}^{13}/\hat{q}^2$ and $\hat{V}^{34}/\hat{q}^2$ by (16) then yields

$$\frac{\hat{V}^{34}}{\hat{q}^2} = \frac{4k_4\mathrm{Ri}T^2(d^{33}-(k_1-2)/(6T))-2k_1T(k_4d^{34}+Td^{44})}{k_1k_3k_4+4\mathrm{Ri}T^2(2k_4+k_1)}, \tag{17a}$$

$$\frac{\hat{V}^{13}}{\hat{q}^2} = \frac{2T(-2k_1Td^{14}+2k_3T(d^{33}-(k_1-2)/(6T))-d^{13})-4(k_1+2k_3)T^2\hat{V}^{34}/q^2}{k_1^2k_3+4\mathrm{Ri}T^2}. \tag{17b}$$

By inserting these relations into (15), this approach reveals that the asymptotic values of T depend on the transport terms d^{ij} and p. These quantities have to be specified in order to obtain T in dependence on the gradient Richardson number Ri.

The same problem of estimating d^{ij} and p was considered by Mellor and Yamada[30] in different studies on the applicability of closures in second-order equations for geophysical fluid problems. They derived a hierarchy of equations: the level 4 model takes all the derivatives d^{ij} into account, the level 3 model neglects all derivatives but d^{44}, the level 2.5 model assumes that $d^{44}=0$, and finally, the level 2 model assumes $p=1$. They note that these levels of models represent decreasing levels of complexity and computational requirements. They found that the level 2.5 model can be applied successfully to solve most of the problems they considered. The approximations of this 2.5 level are applied here also, in order to obtain a robust frequency model for the simulation of complex processes. It is worth emphasizing that the applied approximations are used only for the ω calculation and do not imply, e.g., changes in the structure of the Lagrangian equations (5a) and (5b), where ω appears. This approach differs from that discussed in Sec. III where asymptotic values of d^{ij} are determined through the closure of the equations by the neglect of gradients of third-order terms. There, d^{13} and d^{33} do not vanish but they achieve small stationary values.

When all the d^{ij} are neglected, by inserting expressions (17a) and (17b) into relation (15) one obtains

$$P = \frac{\mathrm{Pr}_t T^2}{\mathrm{Pr}_0 T_0^2} - \frac{\mathrm{Ri}T^2}{\mathrm{Ri}_0 T_0^2}\left\{1+(p-1)\left(1-\frac{\mathrm{Ri}_0}{\mathrm{Pr}_0}\right)\right\}. \tag{18}$$

In this relation $\mathrm{Pr}_t=k_3/k_1[k_1k_3+\mathrm{Ri}_c/\mathrm{Ri}_0\cdot4\mathrm{Ri}T^2]/[k_1k_3+4\mathrm{Ri}T^2]$ is the turbulent Prandtl number $\mathrm{Pr}_t=\mathrm{Ri}\hat{V}^{13}/\hat{V}^{34}$ [this may be seen by inserting (17a) and (17b)] and $T_0^2=3k_1^2/[4(k_1-2)]$ is the value of T^2 under neutral stratification $(\mathrm{Ri}=0)$ for a balanced production–dissipation ratio $p=1$. The numbers Pr_0, Ri_0, and Ri_c are interpreted as flow numbers in the following section. They appear as combinations of the closure parameters k_1, k_3, k_4 and are given by

$$\mathrm{Pr}_0 = \frac{k_3}{k_1}, \tag{19a}$$

$$\mathrm{Ri}_0 = \frac{3}{4T_0^2}\frac{k_1k_3k_4}{k_4(k_1+4)+3k_1}, \tag{19b}$$

$$\mathrm{Ri}_c = \frac{k_3-k_4}{k_4}\frac{\mathrm{Ri}_0}{\mathrm{Pr}_0}. \tag{19c}$$

Inversely, the numbers Pr_0, Ri_c, and Ri_0 determine the closure parameters k_1, k_3, and k_4, since $k_1=[2\mathrm{Pr}_0+3\mathrm{Ri}_c+4\mathrm{Ri}_0+3\mathrm{Ri}_0/\mathrm{Pr}_0]/[\mathrm{Pr}_0-\mathrm{Ri}_0]$, $k_3=\mathrm{Pr}_0k_1$, and $k_4=k_3/[1+\mathrm{Ri}_c\mathrm{Pr}_0/\mathrm{Ri}_0]$.

B. The stationary frequency model

For given p, $\partial U/\partial x^3$, and $\partial\Theta/\partial x^3$, the derived relation (18) represents a quadratic equation for τ^2. The normalized time scale $T=\tau\partial U/\partial x^3$ can be obtained then as a function of p and Ri,

$$\frac{T^2}{T_0^2} = -\frac{\eta\mathrm{Ri}_0-\mathrm{Ri}(\gamma\eta+p\mathrm{Ri}_0)}{2\mathrm{Ri}(\mathrm{Ri}_c-\gamma\mathrm{Ri})}$$

$$+\sqrt{\left[\frac{\eta\mathrm{Ri}_0-\mathrm{Ri}(\gamma\eta+p\mathrm{Ri}_0)}{2\mathrm{Ri}(\mathrm{Ri}_c-\gamma\mathrm{Ri})}\right]^2 + \frac{p\,\eta\mathrm{Ri}_0}{\mathrm{Ri}(\mathrm{Ri}_c-\gamma\mathrm{Ri})}}, \tag{20}$$

where $\gamma=1+(p-1)[1-\mathrm{Ri}_0/\mathrm{Pr}_0]$ and $\eta=[\mathrm{Ri}_c\mathrm{Pr}_0+\mathrm{Ri}_0\times(2\mathrm{Pr}_0+1)]/[\mathrm{Pr}_0-\mathrm{Ri}_0]$ are introduced. Relation (20) can be applied to calculate T provided $\mathrm{Ri}<\mathrm{Ri}_c/\gamma$. This model is denoted the stationary frequency model (SFM).

In Fig. 4, the Ri dependence of T is shown according to (20) for different values p of the production–dissipation ratio of TKE, where the parameters k_1, k_3, and k_3 are set as above. The curves following from the HFM are also presented. For p, the values $p=1.6$ (homogeneous shear flow), $p=1$ (logarithmic boundary layer), and $p=0.4$ (in contrast to $p=1.6$) are chosen. We see that there are no significant differences between the predictions of these models and that
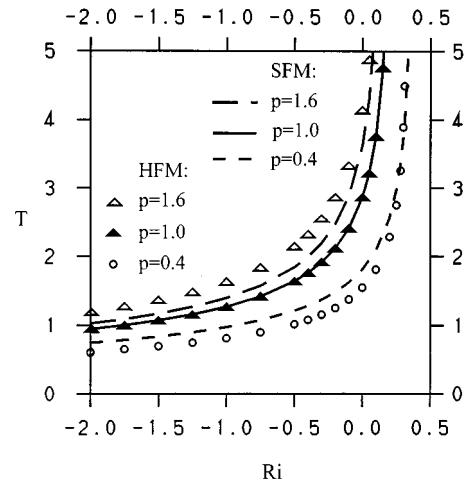

FIG. 4. T in dependence on the gradient Richardson number Ri as calculated by the HFM and the SFM for different values p of the asymptotic production–dissipation ratio of TKE.

they provide the same result for $p = 1$. T becomes infinite at $\text{Ri} \rightarrow \text{Ri}_c / \gamma$, where $\gamma = 1$ for $p = 1$. This curve shows the features discussed in the previous section, i.e., that $T = \tau \partial U / \partial x^3$ becomes smaller with increasing instability of the flow and larger with higher values of the production–dissipation ratio p of TKE. Relation (20) is investigated in more detail in Sec. V, together with an interpretation of the numbers Pr_0, Ri_c, and Ri_0, which appear as parameters in the derived time scale relation.

In order to assess the range of applicability of the neglect of derivatives d^{ij}, let us consider the estimation of T by Eq. (15) for a neutral stratification where no assumptions are made on the d^{ij}. In this case, only d^{13} and d^{33} are unequal to zero and one obtains for T by means of (17a), (17b) and (15),

$$\frac{T}{T_0 \sqrt{p}} = \frac{\sqrt{1 + 3/[(k_1 - 2)p] \cdot (d^{13})^2} - \sqrt{3/[(k_1 - 2)p]} d^{13}}{1 - 6/(k_1 - 2)d^{33}}. \tag{21}$$

Consequently, both a negative d^{13} and a positive d^{33} (as provided by the HFM for $p > 1$; the opposite signs appear for $p < 1$) enlarge T, as may be seen in Fig. 4 at $\text{Ri} = 0$. Their possible influence can be assessed together with that of variations of p.

V. APPLICATION TO ATMOSPHERIC SURFACE LAYER

The predictions of the SFM are compared now with observations in the atmospheric surface layer. This is done in connection with consideration of the parameters k_1, k_3, and k_4 that appear in relation (20) and determine the values of the flow characteristics (Table I). These parameters were estimated by different methods and a multitude of data exists for them, as presented in Table II. In most cases, they are fitted to some of the characteristics of Table I for a neutrally stratified flow,[30] or they are fitted to the characteristics of flows without buoyancy or shear, respectively.[40] In the Lagrangian approach presented in Sec. II, these parameters play a quite different role than they do in second-order closures because there are no other adjustable constants: all the turbulence statistics are determined. Thus, they have to be related to characteristic flow numbers which describe the transition between different scaling regimes. It is shown below that these transitions appear as limit cases of the SFM. The relations obtained provide a link between combinations of second-order closure parameters and flow numbers. The estimation of these characteristic flow numbers is described in Sec. V D.

A. Flow numbers

The existence of characteristic flow numbers related to transitions between flows with different scaling quantities is revealed by considering the relevant time scales. For stratified flow, it can be seen from (18) that the production–dissipation ratio of TKE is determined by $\tau_U = [\partial U / \partial x^3]^{-1}$ and $\tau_\Theta = |\beta g \partial \Theta / \partial x^3|^{-1/2}$, the time scales of forcing by shear and stratification, respectively, and the time scale of dissipation $\tau = q^2 / (2\epsilon)$. One may expect that two characteristic numbers appear in the relations between these time

scales: First, under stable stratification it has to be ensured that the forcing by shear is strong enough for the development of turbulence. Second, under unstable conditions it may be expected that a critical number describes the onset of convective processes (i.e., spatial transport of TKE) with increasing flow instability. Nonstratified flow is then characterized by the turbulent Prandtl number that complements the first two characteristic numbers.

These numbers emerge by considering the relation (18) for a balanced production–dissipation ratio of TKE, $p = 1$. In this case we obtain

$$p = 1 = \left\{ \frac{\text{Pr}_t}{\text{Pr}_0} - \frac{\text{Ri}}{\text{Ri}_0} \right\} \frac{T^2}{T_0^2}, \tag{22}$$

where Ri_c limits the range of applicability of this relation for the calculation of τ by the condition $\text{Ri} < \text{Ri}_c$. The number Pr_0 was explained above to be the turbulent Prandtl number Pr_t under neutral conditions. This number is defined (in the limit $\partial \Theta / \partial x^3 \rightarrow 0$) as the ratio of the contributions (normalized to the corresponding gradients) of production by shear $P_U = -V^{13}(\partial U / \partial x^3)$ and buoyancy production $P_\Theta = \beta g V^{34}$ to the production $P = P_U + P_\Theta$ of TKE,

$$\text{Pr}_0 = \frac{P_U / (\partial U / \partial x^3)^2}{P_\Theta / (-\beta g \partial \Theta / \partial x^3)}. \tag{23}$$

Ri_c appears as the characteristic number for the change of flow properties under stable conditions. Condition (22) cannot be fulfilled for $\text{Ri} > \text{Ri}_c$, i.e., the flow does not reach an asymptotic equilibrium state because the turbulence (i.e., the dissipation) is not strong enough to compensate for the production. In terms of the time scales considered, this condition $\text{Ri} < \text{Ri}_c$ can be written as a constraint for the forcing by shear,

$$\tau_U^2 < \text{Ri}_c \tau_\Theta^2. \tag{24}$$

Because the first term $\text{Pr}_t T^2 / (\text{Pr}_0 T_0^2)$ on the right-hand side of (22) is positive for a positive Pr_t, we obtain from this relation for unstable stratification (with $-\beta g \partial \Theta / \partial x^3 = \tau_\Theta^2$) a condition for the dissipation time scale τ,

$$\tau^2 \leq \text{Ri}_0 T_0^2 \tau_\Theta^2. \tag{25}$$

This relation quantifies the expectation that the dissipation of TKE has to be large enough under unstable conditions for a local transfer of TKE. The equal sign in (25) applies if there is no shear (as given under convective conditions, see below), i.e., $\tau^2 = \text{Ri}_0 T_0^2 \tau_\Theta^2$ for $\partial U / \partial x^3 = 0$. It is worth emphasizing that this relation for unstable flow is characterized by Ri_0 because T_0 represents a normalization of T and is given by its value at neutral stratification, $T_0 = T(\text{Ri} = 0) = \tau / \tau_U$. Hence, Ri_0 determines the onset of convective processes under unstable conditions in analogy to Ri_c, which characterizes the onset of turbulence under stable conditions. This is explained in more detail below, where Ri_0 is shown to characterize the transition between the surface layer and the local free convection layer.[31,45,46]

The parameters Pr_0, Ri_c, and Ri_0 can be estimated by their relations (19a)–(19c) with the closure parameters k_1,

k_3, and k_4. From the data for Pr_0, Ri_c, and Ri_0 given in Table II, ranges of possible values for these numbers can be derived,

$$0.66 < \text{Pr}_0 < 2.36, \tag{26a}$$

$$0.20 < \text{Ri}_c < 0.89, \tag{26b}$$

$$0.11 < \text{Ri}_0 < 0.43. \tag{26c}$$

These values are compared with estimations of these numbers in Sec. V D. First, the predictions of the SFM are shown to be in accord with measured data and the result of the BFM for a neutrally stratified flow with logarithmic mean velocity profile.

B. Turbulence frequency

The obtained dependence of T on the gradient Richardson number is now compared to estimates obtained for the atmospheric surface layer. By applying the definition of τ, T has to be estimated from $T = q^2(\partial U / \partial x^3)/(2\epsilon)$. The quantities on the right-hand side of this relation were measured as functions of $\xi = x^3/L$, where $L = -u_\tau^3/(\kappa \beta g V_0^{34})$ is the Monin–Obuchov length.[46] This quantity determines the ratio of the cubic friction velocity $u_\tau^3 = (-V_0^{13})^{3/2}$ to the vertical heat flux V_0^{34}, where the subscript 0 denotes the values of these fluxes at the surface and κ is the von Kármán constant. The vertical gradient of the horizontal wind was estimated as $\partial U / \partial x^3 = u_\tau/l \, \Phi_M(\xi)$, where l is a mixing length and[47]

$$\Phi_M = \begin{cases} 1 + 4.7\xi, & \text{for } \text{Ri} > 0 \\ (1 - 15\xi)^{-1/4}, & \text{for } \text{Ri} < 0. \end{cases} \tag{27}$$

Different estimations for the dissipation rate exist, for instance, $\epsilon = u_\tau^3/l$ or $\epsilon = u_\tau^3/l[1 + 1/2|\xi|^{2/3}]^{3/2}$.[47] These formulas provide

$$\frac{q^2}{2\epsilon}\frac{\partial U}{\partial x^3} = \frac{1}{2}\left(\frac{q}{u_\tau}\right)^2 \Phi_M(\xi) \begin{cases} 1, & \text{E1} \\ (1 + 1/2|\xi|^{2/3})^{3/2}, & \text{E2}, \end{cases} \tag{28}$$

where E1 refers to the first and E2 to the second expression for ϵ. The results for T are presented in Fig. 5 together with the result of the SFM for $p = 1$. Here, q/u_τ is set to be 2.39 in correspondence with estimations presented by Mellor and Yamada,[30] which gives the same T_0 for all these curves. The parameter ξ can be calculated by the inversion of estimations of Ri in dependence on ξ. One obtains $\xi = \text{Ri}$ for $\text{Ri} < 0$, and for $\text{Ri} > 0$ this relation reads[47]

$$\xi = -\frac{1}{2}\frac{\text{Ri}_c \text{Pr}_0 - \text{Ri}/\text{Ri}_c}{1 - \text{Ri}/\text{Ri}_c}$$

$$+ \sqrt{\frac{1}{4}\left[\frac{\text{Ri}_c \text{Pr}_0 - \text{Ri}/\text{Ri}_c}{1 - \text{Ri}/\text{Ri}_c}\right]^2 + \frac{\text{Ri}\,\text{Ri}_c}{1 - \text{Ri}/\text{Ri}_c}}. \tag{29}$$

Here, the turbulent Prandtl number under neutral stratification is $\text{Pr}_0 = 0.74$ as above and $\text{Ri}_c = 0.21$ is taken as that value where ξ becomes infinite. As can be seen in Fig. 5, the calculated values agree at least qualitatively well with the estimates. All curves become infinite at $\text{Ri} \rightarrow \text{Ri}_c$ but they differ in their asymptotic behavior. For unstable stratification, we find the modeled curve within the range of estimates.
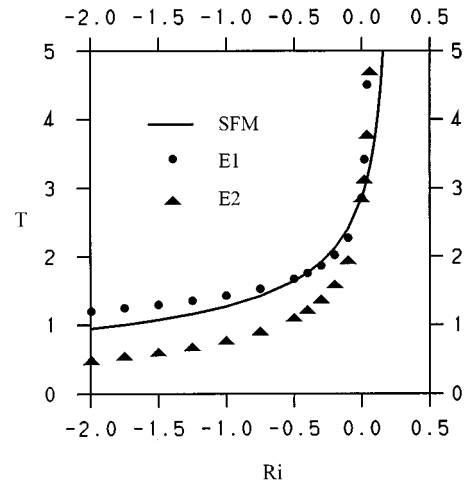

FIG. 5. T in dependence on Ri as calculated by the SFM for $p = 1$. The dots and the triangles correspond to different estimates obtained for the atmospheric surface layer [see Eq. (28)].

In order to reduce the complex dependence of $T(\text{Ri})$, let us develop the relation (20) at $\text{Ri} = 0$. One obtains then (γ and η are given above)

$$T = T_0 p^{1/2}\left[1 - \left(\frac{\gamma}{\text{Ri}_0} + \frac{p}{\eta}\right)\text{Ri}\right]^{-1/2}. \tag{30}$$

This model is denoted the simplified stationary frequency model (SSFM). As shown in Fig. 6 for $p = 1$, there is no important difference between the curve calculated by (20) and this approximation, so that asymptotic frequency calculations can be simplified by applying relation (30).

C. Logarithmic velocity profile

Relation (20) provides the turbulence frequency $\omega = \tau^{-1}$ combined with the shear $\partial U / \partial x^3$. The vertical profile of τ can be obtained then by estimating $\partial U / \partial x^3$, e.g., in a Lagrangian flow model as the gradient of spatial averages
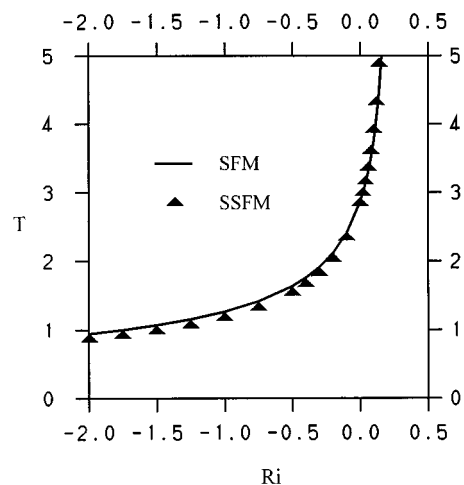

FIG. 6. T calculated in dependence on Ri by the SFM and the SSFM for $p = 1$.

over particle velocities.[7] Let us assume that the logarithmic velocity law is obtained in this way for a neutrally stratified flow, i.e.,

$$U(x^3) = \frac{u_\tau}{\kappa} \ln\left(\frac{x^3}{x_0^3}\right), \tag{31}$$

where x_0^3 is a constant roughness length (u_τ and κ are given above). Then, τ is given according to (20) for $p=1$ as $\tau = T_0(\partial U/\partial x^3)^{-1}$, this means that we find

$$\tau = T_0 \frac{\kappa x^3}{u_\tau} = \sqrt{2T_0^3} \frac{\kappa x^3}{q}, \tag{32}$$

where the second expression for τ is obtained by applying the relation $u_\tau^2 = q^2/(2T_0)$ which follows from the solution of the second-order equation (7). This expression is now compared with the result obtained from the BFM (5). This reads for the conditions in the logarithmic layer

$$\frac{1}{\tau^2}(C_{\epsilon 2} - C_{\epsilon 1}) = \frac{C_\mu \sigma q^2}{2} \frac{\partial}{\partial x^3}\left[\tau \frac{\partial}{\partial x^3} \frac{1}{\tau}\right], \tag{33}$$

because the left-hand side of (5) and ν disappear, $P/\epsilon = 1$, and q^2 is constant.[17] This equation is solved with $\tau = d\tau/dx^3 = 0$ at $x^3 = 0$ by

$$\tau = \sqrt{\frac{2(C_{\epsilon 2} - C_{\epsilon 1})}{C_\mu \sigma}} \frac{x^3}{q} = \sqrt{\frac{2}{C_\mu^{3/2}}} \frac{\kappa x^3}{q}, \tag{34}$$

where the second expression for τ follows from the constraint $C_\mu^{1/2}(C_{\epsilon 2} - C_{\epsilon 1})/\sigma = \kappa^2$ for the coefficients of the BFM, which is required in order to be in consistency with the logarithmic velocity law.[17] We note that the SFM provides for the specified logarithmic velocity law exactly the same result as the BFM if $T_0 = C_\mu^{-1/2}$. The standard value $C_\mu = 0.09$ then leads to $T_0 = 3.33$, which corresponds to $k_1 = 12.4$ (see Sec. IV). This value is greater than the previously applied value $k_1 = 8.3$ for the description of developing anisotropy in a homogeneous shear flow. It does not fall within the range of data presented in Table II. Nevertheless, it corresponds to $C_0 = (k_1 - 2)/3 = 3.5$, which again corresponds to the findings of Du et al., who derived $C_0 = 3.0 \pm 0.5$.[48]

D. Estimation of flow numbers

The flow numbers Ri_c, Pr_0, and Ri_0 can be derived from measurements in the atmospheric surface layer if the limit cases of the scaling quantity $\xi = x^3/L \to \infty$, $\xi \to 0$, and $\xi \to -\infty$ are considered, respectively.

Under stable conditions, Ri_c determines the transition between the surface layer and another layer which is characterized by x^3-less scaling. This layer is found in the upper heights of the stable boundary layer, i.e., $\xi \to \infty$, where local turbulence conditions are completely decoupled from the direct influence of the surface.[31] The increase of ξ with growing stability of the flow (Ri becomes larger) is reflected by relation (29), which gives a fit to measured values. According to this relation, ξ goes to infinity for a critical gradient Richardson number $\mathrm{Ri}_c = 0.21$. This value is found within the ranges $0.21 < \mathrm{Ri}_c < 0.25$ of other estimates where relation (29) appears in a modified form.[46,47] This range is significantly smaller than (26b), which was obtained from the second-order closure parameters.

Under neutral conditions ($\xi \sim 0$), direct measurements of the turbulent Prandtl number Pr_t are presented in Table II, because the value of $k_3 = \mathrm{Pr}_0 k_1$ was calculated by measurements of Pr_0 and estimations of k_1.[30,40] These data give a range of $0.66 < \mathrm{Pr}_0 < 2.36$ for this quantity. The value $\mathrm{Pr}_0 = 0.74$ corresponds to the velocity and potential temperature profiles applied for the derivation of relation (29)[47] and it coincides with the value obtained by LES.[34] However, a value of $\mathrm{Pr}_0 = 1$ is compatible with the results of many investigations.[46]

For highly unstable conditions ($\xi \to -\infty$) Monin–Obuchov scaling fails and has to be replaced by free convective scaling.[46] This limit case permits the estimation of Ri_0. The shear becomes insignificant here and Ri_0 has to be calculated according to (25) by

$$\mathrm{Ri}_0 T_0^2 = \lim_{\xi \to -\infty}\left\{-\beta g \frac{\partial \Theta}{\partial x^3} \frac{q^2}{2\epsilon}\right\}. \tag{35}$$

By adopting Monin–Obuchov scaling we have $-\beta g \partial \Theta/\partial x^3 = \Phi_h(\xi)\beta g V_0^{34}/(\kappa u_\tau x^3)$, where $\Phi_h(\xi)$ has to be fitted to measurements. With the definitions of $L = -u_\tau^3/(\kappa \beta g V_0^{34})$ and $x^3 = \xi L$, this expression can be rewritten to $-\beta g \partial \Theta/\partial x^3 = -\Phi_h(\xi)[\beta g V_0^{34}/u_\tau^2]^2/\xi$. By inserting this expression in (35) we find

TABLE II. The second-order closure parameters k_1, k_2, k_3, and k_4 estimated by different authors and the flow numbers Pr_0, Ri_c, and Ri_0 calculated by means of their relations with the k_1, k_3, and k_4.

	k_1	k_2	k_3	k_4	Pr_0	Ri_c	Ri_0
Wichmann and Schaller[a]	5.0	0.0	3.4	1.48	0.68	0.20	0.11
Mellor and Yamada[b]	6.0	0.08	7.5	1.66	1.25	0.68	0.24
Zeman and Lumley[c]	3.25	0.0	7.0	⋯	2.15	⋯	⋯
André et al.[d]	9.0	0.0	9.7	2.5	1.08	0.85	0.32
Wyngaard et al.[e]	6.7	0.0	4.4	1.4	0.66	0.40	0.12
Yamada[f]	5.0	0.05	11.8	2.0	2.36	0.89	0.43

[a] Reference 40.
[b] Reference 30.
[c] Reference 41.
[d] Reference 42.
[e] Reference 43.
[f] Reference 44.

TABLE III. The normalized time scale T, elements of the anisotropy tensor, and the correlation coefficients calculated by the HFM for different gradient Richardson numbers Ri. In each case, one of the flow numbers $Ri_c = 0.21$, $Pr_0 = 0.74$, and $Ri_0 = 0.25$ is replaced by the value given above, where the other two numbers are left unchanged.

	$Ri_c = 0.7$			$Pr_0 = 0.6$			$Ri_0 = 0.33$		
Ri	-0.25	0	0.13	-0.25	0	0.13	-0.25	0	0.13
T	3.05	4.49	6.15	2.99	4.51	8.11	3.21	4.53	6.82
A^{11}	0.102	0.171	0.213	0.099	0.169	0.235	0.107	0.166	0.220
$-A^{22}$	0.086	0.086	0.086	0.084	0.084	0.084	0.083	0.083	0.083
$-A^{33}$	0.017	0.086	0.128	0.014	0.084	0.151	0.024	0.083	0.137
$-A^{13}$	0.192	0.179	0.151	0.194	0.177	0.125	0.190	0.177	0.143
ρ^{13}	0.517	0.505	0.451	0.521	0.502	0.387	0.514	0.499	0.434
ρ^{14}/r_i	0.636	0.683	0.702	0.941	1.030	1.088	0.866	0.933	0.982
$-\rho^{34}/r_i$	0.698	0.587	0.460	0.898	0.797	0.589	0.884	0.810	0.689
$-V^{34}/V^{14}$	0.936	0.602	0.402	0.820	0.546	0.307	0.856	0.614	0.417

$$Ri_0 T_0^2 = \lim_{\xi \to -\infty} \left\{ -\frac{\Phi_h(\xi)}{4\xi} \left(\frac{q}{u_\tau}(\xi) \right)^4 \right\}, \qquad (36)$$

if $\epsilon = \beta g V_0^{34}$ is applied.[31] The profiles required for the calculation of this limit value are found from the measurements $\Phi_h = \alpha_1 \kappa^{4/3}(-\xi)^{-1/3}$ as well as $(q/u_\tau)^2 = (a_1^2 + 2a_2^2) \times (-\xi)^{2/3}$.[46] With these data we arrive at

$$Ri_0 = \frac{\alpha_1}{4}(a_1^2 + 2a_2^2)^2 C_\mu \kappa^{4/3}, \qquad (37)$$

where $T_0 = C_\mu^{-1/2}$ is used. The values $\alpha_1 = 0.7$, $a_1 = 1.8$, and $a_2 = 1.7$ yield $Ri_0 = C_\mu/0.07\kappa^{4/3}$. This then leads to $Ri_0 = 0.38$ if $\kappa = 0.4$ and $C_\mu = 0.09$ are applied. This value is found within the upper range $0.11 < Ri_0 < 0.43$ of (26c). The derived value in combination with $Pr_0 = 0.74$ and $Ri_c = 0.21$ yields the high value $k_1 = 14.4$. Instead, the choice $Ri_0 = 0.35$ (which can be justified by the approximate estimation of α_1, a_1, and a_2)[46] would be compatible with $k_1 = 12.4$ derived above.

The influence of variations of the flow numbers is presented in Table III. Standard values for k_1, k_3, and k_4 were applied to the comparison of the predictions of the HFM with LES data for homogeneous shear flow (see Sec. III), which correspond to the values $Pr_0 = 0.74$, $Ri_c = 0.21$, and $Ri_0 = 0.25$ for the flow numbers. The results of Kaltenbach $et\ al.$ indicate that the effective critical gradient Richardson number Ri_c/γ equals approximately 0.5 because the flow does not achieve quasisteady states for larger Ri.[34] The definition of this number, Ri_c/γ, in Sec. IV now permits the adjustment of Ri_c to the value 0.7, which leads to $Ri_c/\gamma = 0.5$. The calculated characteristic quantities given in Table I are presented for this value in Table III. We see that the agreement between these values and Tavoularis and Karnik's measured data and the LES data is much better than for $Ri_c = 0.21$. This also applies to the correlation coefficients for the horizontal and vertical heat flux ρ^{14} and ρ^{34}, respectively. Variations of the other two flow numbers ($Pr_0 = 0.63$ has been estimated, e.g., by Rohr $et\ al.$)[38] may lead to similar changes in the T values and the elements of A^{ij} but here the values of ρ^{14} and ρ^{34} are not as satisfactorily obtained as with $Ri_c = 0.7$. This example illustrates the way in which these relations between second-order closure parameters and flow numbers can be used for the adjustment of parameters

to different flows. Here, changes of the flow numbers cause changes in all the characteristics of the flow, in contrast to the effect of variations of closure parameters. In particular, the variations of the flow numbers presented in Table III influence the correlation coefficients ρ^{14} and ρ^{34} in a very different way: These correlations are decreased by the change of Ri_c, increased by the change of Pr_0, and adjusted to each other by the change of Ri_0.

VI. APPLICATION TO BUOYANT PLUME RISE

The explanation of the turbulent mixing between a buoyant (stack) plume and the surrounding fluid is of considerable practical relevance because these mixing effects strongly influence the spatial distribution of plume substances, and their chemical reaction with compounds distributed in the ambient flow. In the Eulerian approach, i.e., based on the conservation equations of mass, momentum, and thermal energy, these mixing processes are described by entrainment and extrainment concepts, as illustrated in Fig. 7.[49] The idea of entrainment of air into plumes by plume-generated turbulence enables the explanation of the two-thirds power law of the buoyant plume rise that is observed in a neutrally stratified flow without significant turbulence.[50,51] For a turbulent flow, the extrainment (i.e., entrainment of plume material into the surrounding fluid due to the ambient turbulence) concept proposed by Netterville permits the calculation of both the leveling-off of the plume and its final height.[49] However, these entrainment and extrainment concepts re-
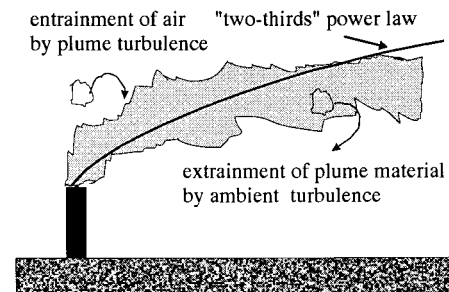

FIG. 7. Illustration of turbulent mixing between a (stack) plume and the ambient flow.

quire the introduction of parameters that cannot be directly derived from measurements and which are not explicitly related to the shear or stratification of the flow (see Sec. VI B).[49,52] This means that the turbulent mixing of plume and ambient fluid particles (its intensity) cannot be scaled in adjustment to variations of the mean velocity and temperature gradients but is handled by ad hoc assumptions. Moreover, the dispersion of plume material (the plume width) cannot be obtained.

In the Lagrangian approach, both the mean plume features and the plume dispersion are described. The dynamics of turbulent mixing is reflected in this approach by the frequencies which appear in the plume particle equations. It was shown by van Dop, that the two-thirds power law of buoyant plume rise and the final height can be explained as consequences of their changes.[28] However, this was also done by means of ad hoc assumptions for these frequencies, so that the scaling of mixing could not be explained. The latter can be achieved if the mixing of plume and ambient flow (i.e., their fluid particles) is indeed simulated by means of a theory of particle motion in accord with turbulence budget equations. This is now demonstrated by applying the stochastic particle equations presented in Sec. II.

The Lagrangian equations for the description of the vertical motion of particles were derived by van Dop.[28] They read

$$\frac{d}{dt}\langle x_L^3 \rangle = \langle U_L^3 \rangle, \tag{38a}$$

$$\frac{d}{dt}\langle U_L^3 \rangle = -\frac{k_1}{4\tau}\langle U_L^3 \rangle + \beta g \langle \Theta_L - \langle \Theta_E \rangle \rangle, \tag{38b}$$

$$\frac{d}{dt}\beta g \langle \Theta_L - \langle \Theta_E \rangle \rangle = -\frac{2k_3 - k_1}{4\tau}\beta g \langle \Theta_L - \langle \Theta_E \rangle \rangle, \tag{38c}$$

if their coefficients are chosen such that these equations are consistent with the second-order equations (2). By neglecting the drift terms $\langle a^i \rangle$ and the mean Eulerian vertical velocity, this can be proved by means of (5a) and (5b) and (6a) and (6b). These equations can be rewritten for a neutral stratification by introducing the normalized particle height $Z = \langle x_L^3 \rangle (\partial U/\partial x^3)^2/B_0$, particle velocity $W = \langle U_L^3 \rangle (\partial U/\partial x^3)/B_0$, and buoyancy $B = \beta g \langle \Theta_L - \langle \Theta_E \rangle \rangle/B_0$, where B_0 is the initial value of $\beta g \langle \Theta_L - \langle \Theta_E \rangle \rangle$ at $t=0$. For a constant shear $\partial U/\partial x^3$ one obtains

$$\frac{dZ}{dt'} = W, \tag{39a}$$

$$\frac{dW}{dt'} = -\frac{k_1}{4T}W + B, \tag{39b}$$

$$\frac{dB}{dt'} = -\frac{2k_3 - k_1}{4T}B, \tag{39c}$$

where the normalized time $t' = t\,\partial U/\partial x^3$ is again applied. The advantage of the here-presented approach of applying Lagrangian equations in consistency with budget equations of turbulence consists essentially in the estimation of the

(normalized) particle frequencies $k_1/4T$ and $(2k_3-k_1)/4T$ in terms of the (normalized) turbulence frequency T^{-1}. The time behavior of this frequency is described by the HFM (11) with $p=1.6$ as for an homogeneous shear flow. The implications of this assumption are considered below and compared with the results of previously applied methods.

A. Nonturbulent flow

First, we consider buoyant plume rise in a neutrally stratified and nonturbulent ambient flow. This case is relevant to the initial stage of plume rise where the influence of the ambient turbulence can be neglected (the entrainment stage) and for a calm ambient turbulence. In the frequency equation (11), this case is described by the first term on the right-hand side. The second and third terms vanish ($\partial U/\partial x^3 \to 0$ for the unsheared turbulence and V^{34} is zero due to the neutral stratification) and we obtain as a solution of the equation system (39a)–(39c) combined with (7) and (11) and the initial conditions $Z(t=0)=0$, $W(t=0)=0$, and $B(t=0)=1$ the normalized height Z over the source as

$$Z = \frac{I^{2-m_1}}{(C_{\epsilon 2}-1)^2(m_1-m_2)}\left\{\frac{(I+(C_{\epsilon 2}-1)t')^{m_1}-I^{m_1}}{m_1}\right.$$
$$\left. - \frac{(I+(C_{\epsilon 2}-1)t')^{m_2}-I^{m_2}}{m_2}I^{m_1-m_2}\right\}, \tag{40}$$

where the abbreviations $m_1 = 2-(2k_3-k_1)/4(C_{\epsilon 2}-1)$ and $m_2 = 1-k_1/4(C_{\epsilon 2}-1)$ are used and I gives the initial value of T as above.

For $t' \to \infty$, this curve approaches (provided $m_2 < m_1$ as usually given with standard values for these parameters)

$$Z = \frac{1}{m_1(m_1-m_2)}\left(\frac{I}{C_{\epsilon 2}-1}\right)^{2-m_1}t'^{m_1}, \tag{41}$$

if I is neglected with respect to t' and only the highest power of t' is taken into account. By applying the definitions of Z, I, and t', the mean particle height over the source is obtained as

$$\langle x_L^3 \rangle = \frac{B_0 \tau_0^2}{m_1(m_1-m_2)(C_{\epsilon 2}-1)^{2-m_1}}\left(\frac{t}{\tau_0}\right)^{m_1}, \tag{42}$$

where τ_0 is the initial value of τ, $\tau_0 = \tau(t=0)$. This expression corresponds to the two-thirds power law[49–51] when $m_1 = 2/3$, i.e.,

$$C_{\epsilon 2} = 1 + \frac{3k_1}{8}\left(\mathrm{Pr}_0 - \frac{1}{2}\right). \tag{43}$$

The similarity behavior of the buoyant plume rise appears as a consequence of explaining buoyant turbulence as stochastic particle motion and adopting the HFM (which corresponds here to Kolmogorov's original frequency equation, without the spatial transport terms),[22] provided that this consistency constraint (43) is fulfilled between the parameter $C_{\epsilon 2}$ of the dissipation model and the parameters of the turbulence model. The values applied above, $C_{\epsilon 2} = 1.9$ and $k_1 = 8.3$, lead to $\mathrm{Pr}_0 = 0.79$, which is rather close to the assumed $\mathrm{Pr}_0 = 0.74$.

This power law can also be deduced in the Eulerian framework from conservation equations of mass, momentum, and thermal energy by means of the entrainment assumption.[49–51] This approach provides

$$\langle x_L^3 \rangle = \left(\frac{3F_0}{2\beta_P^2 U_0} \right)^{1/3} t^{2/3}, \qquad (44)$$

where F_0 is the initial plume buoyancy, U_0 is the horizontal mean velocity at source height, and β_P is the plume entrainment constant (which is usually denoted β[49,51] but is written here in accordance to β_T, see below). Usually, $\beta_P = 0.6$ is assumed,[51] but the use of $\beta_P = 0.65$ is also supported by measurements.[49] Comparison of the coefficients of (42) and (44) shows that the asymptotic behavior is the same in these approaches when β_P is determined by

$$\beta_P = \frac{C_\beta}{\tau_0^2} \sqrt{\frac{F_0}{B_0^3 U_0}} = C_\beta \frac{R_0}{B_0 \tau_0^2}, \qquad (45)$$

where the definitions of I and (in the last expression on the right-hand side) $F_0 = U_0 B_0 R_0^2$ are applied. R_0 gives the radius of the active plume at the end of the bending-over phase.[49] Additionally, the abbreviation

$$C_\beta = \frac{2}{3} (C_{\epsilon 2} - 1)^2 \left(1 + \frac{k_1(1 - \mathrm{Pr}_0)}{2(C_{\epsilon 2} - 1)} \right)^{3/2} \qquad (46)$$

is used in (45), where $C_\beta = 3/2$ is found with the values for the parameters given above. We see that β_P is found to be proportional to the ratio of the length scale R_0 of the plume width at the end of the bending-over stage to the length scale $B_0 \tau_0^2$ of the mean plume height, i.e., it gives a measure for the intensity of the plume-generated turbulence. The value $\beta_P = 0.66$ (which is very near to $\beta_P = 0.65$ as derived by Netterville)[49] is found for the entrainment constant if the diameter of the active plume is assumed to be equal to the mean plume height over the source in the bending-over stage at $t = \tau_0$, i.e., $2R_0 = \langle x_L^3 \rangle$, where $\langle x_L^3 \rangle = 0.875 B_0 \tau_0^2$ is found through (42). The curve (40) that follows for a nonturbulent flow (the shear in the normalizations of Z and t' compensate each other) from the solution of (39a)–(39c) combined with (7) and (11) is presented in Fig. 8. Asymptotically, this curves coincides with the two-thirds power law given by (41). For the Nanticoke plume rise measurements, $\tau_0 = 4.3$ s is deduced from the estimations of F_0, U_0, and B_0.[49] For the wind shear $\partial U / \partial x^3 = T_\infty / \tau_\infty = 0.04$ s^{-1} is found by adopting a value of $\tau \cong 100$ s for the ambient turbulence[28] and applying $T_\infty \cong 4$ (see Sec. III). This leads to the initial value $I = \tau_0 \partial U / \partial x^3 = 0.172$ of T that is applied to the calculation of the curves presented in Fig. 8.

B. Turbulent flow

For a turbulent flow with nonvanishing shear, one observes that the plume levels off and reaches a final plume height (the dashed line in Fig. 8). This is the result of extrainment (see Fig. 7) and is described by the second and third terms on the right-hand side of (11), where the influence of the ambient turbulence is reflected by the normalized variances. The final plume rise is found to be
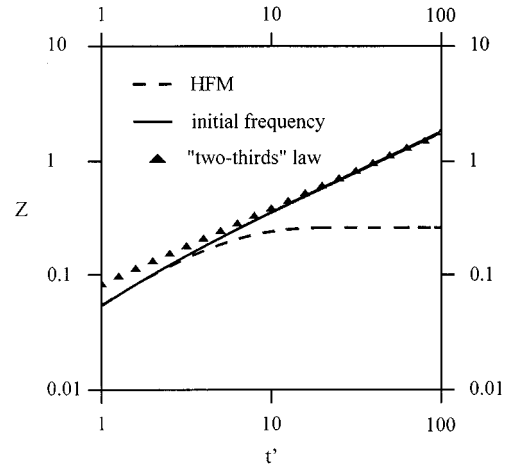

FIG. 8. The normalized height Z as function of t' as obtained by the HFM. The solid curve represents the curve (40), which is found for a nonturbulent flow. The dashed curve shows the result for a turbulent flow. The triangles represent the observed two-thirds power law of the buoyant plume rise.

$$\langle x_L^3 \rangle_\infty = 1.838 I \lambda(I) \frac{B_0}{(\partial U / \partial x^3)^2}, \qquad (47)$$

where the asymptotic value of Z is calculated numerically. Curve $\lambda(I)$ is presented in Fig. 9. Adopting the data of the Nanticoke experiments, $B_0 = 0.764$ m s^{-2} and the other quantities given above (leading to $\lambda = 0.77$), one obtains for the final plume height $\langle x_L^3 \rangle = 116$ m. This agrees fairly well with $\langle x_L^3 \rangle = (119 \pm 40)$ m as found in the Nanticoke experiments. This final plume height goes to infinity for a nonturbulent ambient flow, $\partial U / \partial x^3 \to 0$, because $\lambda(I) \to 0.4$ and, consequently, $\langle x_L^3 \rangle = 0.735 B_0 \tau_0 / (\partial U / \partial x^3)$.

In the Eulerian approach,[49] the extrainment concept leads to a final plume height of

$$\langle x_L^3 \rangle_\infty = \left\{ \frac{3F_0}{\beta_P^2 U_0 f^2} \right\}^{1/3}, \qquad (48)$$
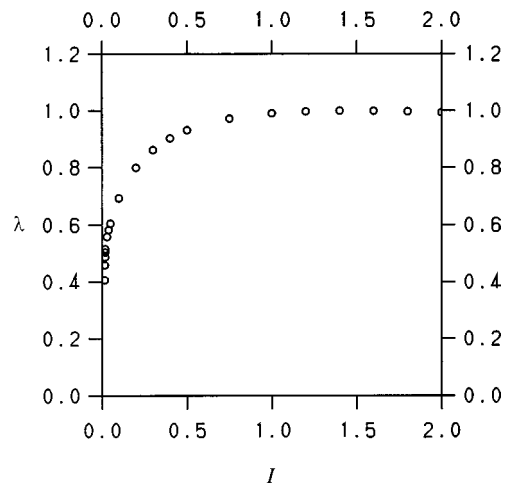

FIG. 9. The factor λ in Eq. (47) in dependence on the initial normalized time scale I.

where a turbulence buffet frequency $f = 2\beta_P i_E U_0 / \Lambda_E$ is introduced. Here, i_E is the intensity of turbulence and Λ_E is the length scale of large-scale eddies. By comparing this expression with (47) one finds that both approaches provide the same final value if

$$f = \beta_T \frac{\partial U}{\partial x^3}, \tag{49}$$

where (45) is applied and $\beta_T = 0.7 I^{1/2} / (C_\beta \lambda^{3/2}(I))$ is introduced. Hence, the simulation of the turbulent mixing between plume and ambient flow particles in the Lagrangian approach permits the explicit calculation of the turbulence buffet frequency f, so that the dependence of the mixing on shear is obtained. In contrast, the mixing intensity is described in the Eulerian expression for f by $i_E U_0 / \Lambda_E$, which cannot be directly derived from measurements. The quantity β_T is the parameter of the extrainment stage corresponding to the parameter β_P of the entrainment stage. It is determined by the ratio of the plume time scale τ_0 to that of the ambient turbulence $\tau_U = (\partial U / \partial x^3)^{-1}$. The value $I = 0.172$ applied above leads to $\beta_T = 0.29$. The appearance of β_P in the Eulerian expression results from the assumption that these two parameters β_T and β_P are proportional to each other.

VII. SUMMARY

Stochastic particle models of buoyant turbulence enable an understanding of turbulent mixing effects, as demonstrated in Sec. VI. The scaling of mixing (its dependence on shear and stratification) depends in these models on the characteristic turbulence frequency ω, for which here different models have been considered. The presented HFM (11) describes the time behavior and the asymptotic values of ω in accord with LES data for stratified homogeneous shear flows. This model is coupled with a second-order closure model for the turbulence through the production–dissipation ratio of TKE. A decoupling of this model (as is usually done for neutrally stratified flow) leads to the SHFM (14) discussed in Sec. III. This model predicts the ω behavior of neutrally and unstably stratified flow similar to the HFM. For stably stratified flow, the differences between the HFM and the SHFM become greater with growing stability. The SFM (20) provides analytically the stationary spatial patterns of ω similar to the HFM. This model can be simplified remarkably to the SSFM (30), as demonstrated in Sec. V. The SFM and the HFM are applied to the description of transitions between turbulent flow regimes in the stationary atmospheric surface layer and to buoyant plume rise, respectively.

The SFM has been shown to be in accord with estimates obtained for the atmospheric surface layer. For a given logarithmic mean velocity profile, we demonstrated in Sec. V C that its predictions agree with those of the BFM (3). Limit cases of this model describe transitions between different scaling regimes in the atmospheric surface layer and provide links between closure parameters and flow numbers that characterize these transitions. Here, we have introduced a new flow number Ri_0 that describes the transition to free convective flow under unstable stratification in analogy to the critical gradient Richardson number, Ri_c, which deter-

mines the onset of turbulence under stable stratification (see Sec. V D). The calculation of model parameters through estimations of these flow numbers offers various advantages: (i) these connections provide insight into the limits of the applicability of second-order closures (given by the derived laminarization and convection limits for stably and unstably stratified flow, respectively), (ii) the parameter variation is explained for different turbulent flows (a possible range of values can be assessed directly), and (iii) the variation of flow numbers offers new possibilities for the adjustment of model parameters to special flow properties, as illustrated in Sec. V D.

By applying the HFM, a new theory is presented for buoyant plume rise, which is explained as the result of the turbulent motion of fluid particles of the plume and ambient flow as well as the change of their temperatures. This permits the calculation of the entrainment and extrainment parameters β_P and β_T that reflect the effects of turbulent mixing by plume-generated and ambient turbulence, respectively, in terms of the relevant time (or length) scales. Consequently, the dynamic behavior of buoyant plume rise can be explained without ad hoc assumptions. For a neutrally stratified and nonturbulent flow, the two-thirds power law is derived and for a turbulent flow the plume's leveling-off is found to be in agreement with measurements in the atmosphere. Buoyant plume rise simulations which apply the theory presented here offer considerable advantages over other methods: (i) mean plume rise and dispersion can be calculated consistently, (ii) the (possibly large) variations of the mixing intensity are explained only by measurable quantities in dependence on shear and stratification, which enables in particular (iii) accurate calculations of chemical transformations in reactive plumes (or in any other buoyant flows) where the knowledge of the mixedness of species is essential.

[1] S. B. Pope, ''PDF methods for turbulent reactive flows,'' Prog. Energy Combust. Sci. **11**, 119 (1985).
[2] H. van Dop, F. T. M. Nieuwstadt, and J. C. R. Hunt, ''Random walk models for particle displacements in inhomogeneous unsteady turbulent flows,'' Phys. Fluids **28**, 1639 (1985).
[3] D. J. Thomson, ''Criteria for the selection of stochastic models of particle trajectories in turbulent flows,'' J. Fluid Mech. **180**, 529 (1987).
[4] S. B. Pope, ''Computations of turbulent combustions: Progress and challenges,'' *23rd Symposium (International) on Combustion* (The Combustion Institute, Pittsburgh, PA, 1991), pp. 591–612.
[5] B. L. Sawford, ''Recent developments in the Lagrangian stochastic theory of turbulent dispersion,'' Boundary-Layer Meteorol. **62**, 197 (1993).
[6] S. B. Pope, ''Lagrangian PDF methods for turbulent flows,'' Annu. Rev. Fluid Mech. **26**, 23 (1994).
[7] S. B. Pope, ''Particle methods for turbulent flows: Integration of stochastic model equations,'' J. Comput. Phys. **117**, 332 (1995).
[8] R. O. Fox, ''Computational methods for turbulent reacting flows in the

chemical process industry,'' Rev. Inst. Francais du Pétrole **51**, 215 (1996).

[9] J. D. Wilson and B. L. Sawford, ''Review of Lagrangian stochastic models for trajectories in the turbulent atmosphere,'' Boundary-Layer Meteorol. **78**, 191 (1996).

[10] S. B. Pope, ''On the relationship between stochastic Lagrangian models of turbulence and second-moment closures,'' Phys. Fluids **6**, 973 (1994).

[11] P. A. Durbin and C. G. Speziale, ''Realizability of second-moment closure via stochastic analysis,'' J. Fluid Mech. **280**, 395 (1994).

[12] H. A. Wouters, T. W. J. Peeters, and D. Roekaerts, ''On the existence of a generalized Langevin model representation for second-moment closures,'' Phys. Fluids **8**, 1702 (1996).

[13] S. Heinz, ''Nonlinear Lagrangian equations for turbulent motion and buoyancy in inhomogeneous flows,'' Phys. Fluids **9**, 703 (1997).

[14] R. O. Fox, ''The spectral relaxation model of the scalar dissipation rate in homogeneous turbulence,'' Phys. Fluids **7**, 1082 (1995).

[15] S. B. Pope and Y. L. Chen, ''The velocity-dissipation probability density function model for turbulent flows,'' Phys. Fluids A **2**, 1437 (1990).

[16] S. B. Pope, ''Application of the velocity-dissipation probability density function to inhomogeneous turbulent flows,'' Phys. Fluids A **3**, 1947 (1991).

[17] D. C. Wilcox, *Turbulence Modeling for CFD* (DCW Industries, La Cañada, CA, 1993).

[18] J. L. Lumley, *Whither Turbulence? Turbulence at the Crossroads* (Springer, Berlin, 1990).

[19] D. C. Wilcox, ''Reassessment of the scale determining equations for advanced turbulence models,'' AIAA J. **26**, 1299 (1988).

[20] J. Xu and S. B. Pope, ''Sources of bias in particle-mesh methods for PDF models for turbulent flows,'' FDA-Report No. 97-01, Cornell University, 1997.

[21] S. Heinz, A. Cadiou, and K. Hanjalić, ''Turbulent energy transport in non-neutral shear flows,'' 11th Symposium on Turbulent Shear Flows, Grenoble, France, 1997, pp. 2313–2318.

[22] A. N. Kolomogorov, ''Equations of turbulent motion of an incompressible fluid,'' Izv. Akad. Nauk SSSR, Ser. Fiz. **6**, 56 (1942).

[23] J. C. Rotta, ''Statistische theorie nichthomogener turbulenz,'' Z. Phys. **129**, 547 (1951).

[24] B. E. Launder, ''On the effects of a gravitational field on the turbulent transport of heat and momentum,'' J. Fluid Mech. **67**, 569 (1975).

[25] T. J. Craft, N. Z. Ince, and B. E. Launder, ''Recent developments in second-moment closure for buoyancy-affected flows,'' Dyn. Atmos. Oceans **23**, 99 (1996).

[26] B. E. Launder, ''Progress and prospects in phenomenological turbulence models,'' in *Theoretical Approaches to Turbulence*, edited by D. L. Dwoyer, M. Y. Hussaini, and R. G. Voight (Springer, New York, 1985), p. 155.

[27] K. Hanjalić, ''Advanced turbulence closure models: A view of current status and future prospects,'' Int. J. Heat Fluid Flow **15**, 178 (1994).

[28] H. van Dop, ''Buoyant plume rise in a Lagrangian framework,'' Atmos. Environ. **26A**, 1335 (1992).

[29] C. G. Speziale and T. B. Gatski, ''Assessment of second-order closure models in turbulent shear flows,'' AIAA J. **32**, 2113 (1994).

[30] G. L. Mellor and T. Yamada, ''Development of a turbulence closure model for turbulent flows,'' Rev. Geophys. Space Phys. **20**, 851 (1982).

[31] F. T. M. Nieuwstadt and P. G. Duynkerke, ''Turbulence in the atmospheric boundary layer,'' Atmos. Res. **40**, 111 (1996).

[32] W. P. Jones and B. E. Launder, ''The prediction of laminarization with a two-equation model of turbulence,'' Int. J. Heat Mass Transf. **15**, 301 (1972).

[33] B. E. Launder and D. B. Spalding, *Mathematical Models of Turbulence* (Academic, New York, 1972).

[34] H. J. Kaltenbach, T. Gerz, and U. Schumann, ''Large-eddy simulation of homogeneous turbulence and diffusion in stably stratified flows,'' J. Fluid Mech. **280**, 1 (1994).

[35] T. Gerz, U. Schumann, and S. E. Elghobashi, ''Direct numerical simulation of stratified homogeneous turbulent shear flows,'' J. Fluid Mech. **200**, 563 (1989).

[36] S. Tavoularis and U. Karnik, ''Further experiments on the evolution of turbulent stresses and scales in uniformly sheared turbulence,'' J. Fluid Mech. **204**, 457 (1989).

[37] C. A. G. Webster, ''An experimental study of turbulence in a density stratified shear flow,'' J. Fluid Mech. **172**, 17 (1964).

[38] J. J. Rohr, E. C. Itsweire, K. N. Helland, and C. W. van Atta, ''Growth and decay of turbulence in a stably stratified shear flow,'' J. Fluid Mech. **195**, 77 (1988).

[39] A. J. Ley and D. J. Thomson, ''A random walk model of dispersion in the diabatic surface layer,'' Q. J. R. Meteorol. Soc. **109**, 847 (1983).

[40] M. Wichmann and E. Schaller, ''On the determination of the closure parameters in high-order closure models,'' Boundary-Layer Meteorol. **37**, 323 (1986).

[41] O. Zeman and J. L. Lumley, ''Modeling buoyancy driven mixed layer,'' J. Atmos. Sci. **33**, 1974 (1976).

[42] J. C. André, G. De Moor, P. Lacarrére, G. Therry, and R. du Vachat, ''Modeling the 24-hour evolution of the mean and turbulent structures of the planetary boundary layer,'' J. Atmos. Sci. **35**, 1861 (1978).

[43] J. C. Wyngaard, O. R. Coté, and K. S. Rao, ''Modeling the atmospheric boundary layer,'' Adv. Geophys. **18A**, 193 (1974).

[44] N. Yamada, ''Model for the pressure terms in the equation for second-order turbulence moments,'' J. Meteorol. Soc. Jpn. **63**, 695 (1985).

[45] A. A. M. Holtslag and F. T. M. Nieuwstadt, ''Scaling the atmospheric boundary layer,'' Boundary-Layer Meteorol. **36**, 201 (1986).

[46] J. R. Garratt, *The Atmospheric Boundary Layer*, Cambridge Atmospheric and Space Science Series (Cambridge University Press, Cambridge, 1992).

[47] R. B. Stull, *An Introduction to Boundary Layer Meteorology* (Kluwer, Dordrecht, 1988).

[48] S. Du, B. L. Sawford, J. D. Wilson, and D. J. Wilson, ''Estimation of the Kolmogorov constant (C_0) for the Lagrangian structure function, using a second-order Lagrangian model of grid turbulence,'' Phys. Fluids **7**, 3083 (1995).

[49] D. D. Netterville, ''Plume rise, entrainment and dispersion in turbulent winds,'' Atmos. Environ. **24A**, 1061 (1990).

[50] G. A. Briggs, ''Plume Rise Predictions,'' Lectures on air pollution and environmental impact analyses, AMS, 1975, pp. 59–111.

[51] J. C. Weil, ''Plume rise,'' in *Lectures on Air Pollution Modeling*, edited by A. Venkatram and J. C. Wyngaard (American Meteorological Society, Boston, 1988), pp. 119–166.

[52] G. Gangoiti, J. Sancho, G. Ibarra, L. Alonso, J. A. García, M. Navazo, N. Durana, and J. L. Ilardia, ''Rise of moist plumes from tall stacks in turbulent and stratified atmospheres,'' Atmos. Environ. **31A**, 253 (1997).